Preparation of mesoporous silica (MCM41) and its use as an adsorbent for heavy metals for acid mine drainage

T. Falayi[1], F. Ntuli[2] & Z. B. Sithole[2]
[1]*Department of Civil Engineering Sciences, University of Johannesburg, South Africa*
[2]*Department of Chemical Engineering, University of Johannesburg, South Africa*

Abstract

Potassium silicate solutions obtained were used as a source for MCM41. The preparation of MCM41 was affected by the gelation pH. A pH of 7 produced the purest MCM41 with an external surface area of 98,000 $m^2 m^{-3}$. The MCM41 could be used as an adsorbent for heavy metals in AMD. A 4% m/v solid loading of MCM41 could remove 95.5, 97.3 and 99.6% of Ni, Cu and Fe respectively. The adsorption process was found to fit the Langmuir isotherm and pseudo second order kinetics. The Gibbs free energy of adsorption for all metals was below -20 kJ/mol for all metals. The enthalpy for Fe, Cu and Ni removal were 19.97, 21.40 and 16.44 kJ/mol respectively and thus endothermic. The entropy for the removal of Fe, Cu and Ni were found to75.6, 76.2 and 56.5 J/mol respectively showing the strong affinity of MCM41 for the metals. The process was also thermodynamically spontaneous with the spontaneity increasing with an increase in temperature.
Keywords: MCM41, adsorption, heavy metals, isotherm.

1 Introduction

In South Africa low-grade brown coal is used for electricity generation and fly ash (FA) remains as a waste product [1]. FA is pollutant since it is contaminated by a lot of heavy metals including arsenic, lead, mercury, cadmium only to name a few [2]. Extraction of silica from FA has been studied and is an attractive alternative

WIT Transactions on Ecology and The Environment, Vol 210, © 2016 WIT Press
www.witpress.com, ISSN 1743-3541 (on-line)
doi:10.2495/SDP160671

in FA waste management which might lead to the full utilisation of FA [3, 4]. The silicate solutions can also be used to produce silica xerogels and MCM41 [3, 4]. The production of MCM41 as an adsorbent for heavy metals therefore provides an alternative to use a waste material to treat another waste stream. Acid mine drainage is acidic water laden with a high sulphate and metal content. AMD results when water is exposed to air in the presence of pyritic rock left by mining activities. Currently AMD is one of the major concerns in South Africa [5]. This paper therefore deals with the parameters affecting preparation of MCM41 from potassium silicate solution. The effect of gelation pH and ageing time are discussed. The use of prepared MCM41 as an adsorbent for heavy metals in acid mine drainage (AMD) is also discussed. The adsorption isotherm, kinetics and thermodynamic parameters of the heavy metals adsorption using MCM41 was also investigated.

2 Experimental

Batch preparation of MCM41 was done using cetyltri-methyl ammonium bromide (CTAB) and ethyl acetate ($CH_3COOC_2H_5$). Batch adsorption experiments were also done.

2.1 Materials

Potassium silicate solution was obtained from leaching of FA. HCl, $C_{16}H_{33}(CH_3)_3NBr$ (cetyltri-methyl ammonium bromide), $CH_3COOC_2H_5$, KOH and HNO_3 were supplied by supplied by Rochelle Chemicals South Africa.

2.2 Equipment

A Rigaku ZSX Primus II XRF was used for oxide content determination of MCM41. Mineralogical analysis was done using a Rigaku Ultima IV difractometer. Metal analysis was achieved using an Atomic Absorption Spectrometer (AAS) (Thermo scientific ICE 3000 Series).

2.3 Preparation of MCM41

Sulica was extracted from FA using prior experimental work by the authors [6]. The silicate solution was then concentrated by evaporation. The concentrated solution was then used to prepare MCM41. MCM41 source solution was prepared at 85°C and under stirring at 200 rpm. 300 ml of the concentrated potassium silicate solution was mixed with 3 g of CTAB to obtain an aqueous solution. Then, under stirring at 500 rpm, 9.3 ml of ethyl acetate was rapidly added to the solution. After stirring the mixture for 10 min, the obtained solution was cooled down to room temperature (25°C) by natural convection [3]. The solution was named as MCM41 solution.

50 ml of MCM41 solution was adjusted to a pH of 3, 5, 7, 9 and 11 respectively by the addition of 5 N H_2SO_4 solutions under slow stirring (50 rpm). Precipitation was observed during pH adjustment. The pH adjusted solution with the

precipitated MCM41 was aged at room temperature (25°C) for 24 h. The materials obtained was then washed with deionised water till the washing water was at a pH of 7 and dried at 100°C for 2 h. The dried material (MCM41 was then analysed using laser diffraction, XRF and XRD.

2.4 Effect of MCM41 solid loading on adsorption of heavy metals

1–5 g of MCM41 prepared at the pH of 7 was added to a separate 100 ml solutions of AMD. The solutions were agitated at 200 rpm using a thermostatic shaker maintained at 25°C for 2 h. After 2 h the agitation was stopped and the solution pH was measured. The solutions were then filtered using vacuum filtration. The filtrate was then acid digested before metal analysis using AAS.

2.5 Effect of residence time on the adsorption of heavy metals

4 solutions of 100 ml AMD mixed with 4 g each of MCM41 were prepared. The solutions were agitated at 200 rpm using a thermostatic shaker maintained at 25°C for 30, 60, 90 and 120 min respectively. At the end of each agitation time the solution pH was measured. The solutions were then filtered using vacuum filtration. The filtrate was then acid digested before metal analysis using the AAS. The above procedure was repeated at 35°C and 45°C to see the effect of temperature on the adsorption of heavy metals.

2.6 Metal analysis

Sample digestion was achieved by quantitatively transferring 100 ml of AMD sample to a 250 ml volumetric flask. The sample was then acidified with 2 ml of 1:1 HNO_3: H_2O and 1 ml of 1:1 HCl:H_2O. The volumetric solution was then covered by a slightly raised watch glass and placed on a hot plate to provide evaporation at not more than 80°C. The volume of the sample was then reduced to about 20 ml by evaporation. After cooling, 20 ml of the digested sample was quantitatively transferred to a 50 ml volumetric flask and made up to volume with Reverse Osmosis (RO) water. The sample was then ready for AAS analysis. The calibration standards were prepared by appropriate dilution of the 100 ppm stock solutions of each respective metal analysed.

3 Results and discussion

3.1 Effect of gelation pH on XRF analysis

Table 1 shows the XRF analysis of MCM41 which was precipitated at various pH.

More alumina was incorporated into MCM41 as the pH increased. This was because at lower pH the alumina remained in solution. The increase in alumina has been thought to be due to the lower polycondensation degree of the silicate species which leads to higher incorporation of the alumina species [6].

Table 1: XRF analysis of MCM41.

Constituent	Different pH levels				
	3	5	7	9	11
Al_2O_3	5.40	10.60	2.50	20.40	20.38
SiO_2	10.80	40.20	80.60	68.78	50.25
P_2O_5	0.01	0.99	0.12	0.03	0.01
SO_3	48.26	30.65	1.25	4.25	20.65
Cl	0.01	0.02	0.02	0.02	0.01
K_2O_3	35.48	17.50	15.44	6.50	8.65
Fe_2O_3	0.03	0.04	0.06	0.02	0.04

3.2 Effect of gelation pH on surface area of MC M41

The external surface area was calculated from the PSD generated by laser diffraction by first transforming the volume distribution to a number density distribution and then using the method of moments to calculate the second moment (*m2*-equivalent to external surface area) [7]. Figure 1 shows the number distribution and Table 2 shows the variation of external surface area with gelation pH.

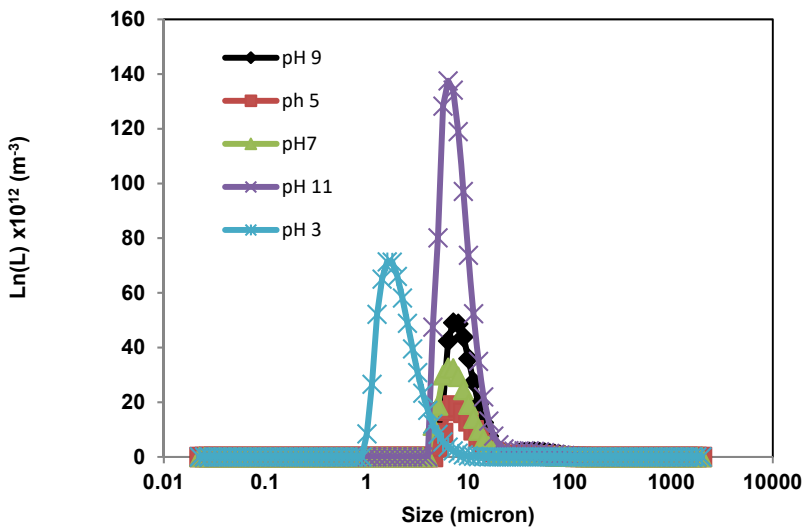

Figure 1: Variation of number distribution with pH.

There was an increase in particle size with an increase in pH. It has been shown that silica precipitation starts at pH less than 10 [8] and therefore primary particles increase in size and decrease in number as a result of the Oswald ripening process as shown in Figure 1. This is further supported by the decrease in external surface area (as shown in Table 2).

Table 2: Variation of external surface area with pH.

pH	3	5	7	9	11
External surface area ($\times 10^3$ m^2 m^{-3})	3099	110	98	26	0.72

The increase in particle size resulted in reduction in external surface area. The MCM41 produced at pH 7 was then chosen for adsorption experiments as it had the highest purity of silica (Table 1) and a reasonably large external surface area.

3.3 Analysis of AMD

Table 3 shows the heavy metal content of the AMD. Fe, Ni and Cu were of particular interest.

Table 3: Characterisation of AMD.

Parameter	Concentration (ppm)
Fe	500
Ni	50
Cu	50
pH	2.67

The AMD metal concentrations were above the statutory limits for water discharge in South Africa.

3.4 Effect of MCM41 solid loading on adsorption of heavy metals

Figure 2 shows the variation in metal removal with solid loading.

There was an increase in metal removal with an increase in solid loading. This is due to increase in available adsorption sites. There was no statistical difference in metal removal at 4 and 5%. Therefore 4% solid loading was chosen for subsequent experiments. 4% solid loading resulted in 99.8, 97.4 and 95.7% in Fe, Cu and Ni removal.

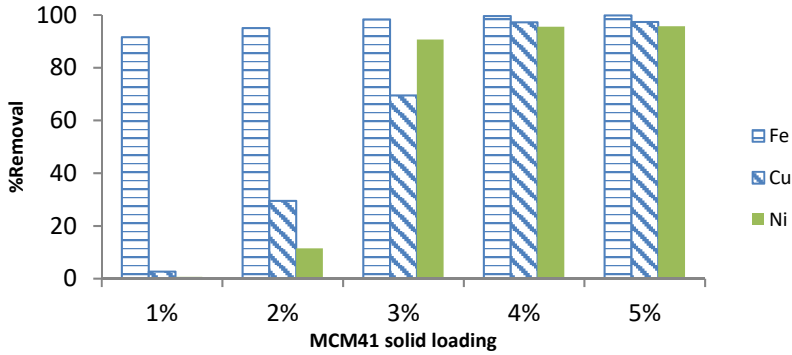

Figure 2: Variation in metal removal with solid loading.

3.5 Effect of residence time on the removal of metals

Figure 3 shows the variation in metal removal with time.

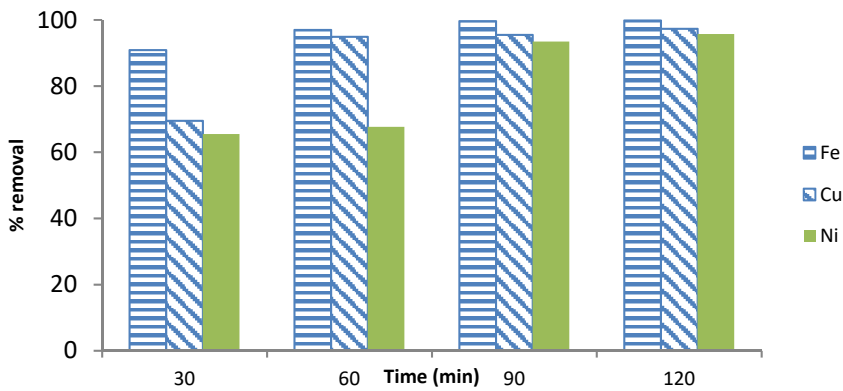

Figure 3: Variation of metal removal with time at 4% solid loading.

There was an increase in metal removal with time. The increase in metal removal was due to increased contact time between MCM41 with the AMD. There was no statistical difference in metal removal between 90 and 120 min. This showed that the equilibrium was reached between 90 and 120 min.

3.6 Adsorption isotherms

The metal removal data was fitted into Langmuir and Freundlich isotherms. Figures 4 and 5 show the Langmuir and Freundlich plots respectively.

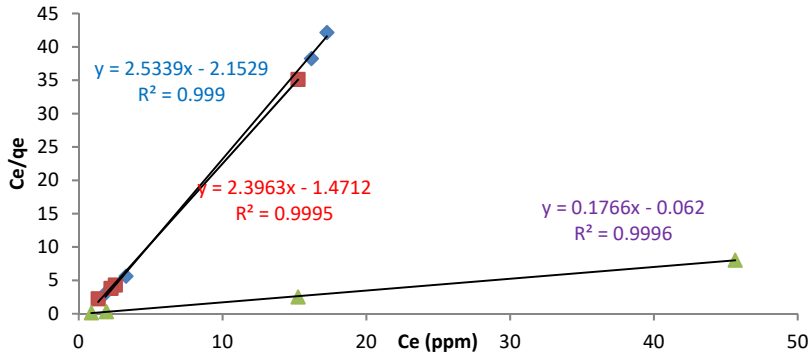

Figure 4: Langmuir plot for Fe, Ni and Cu.

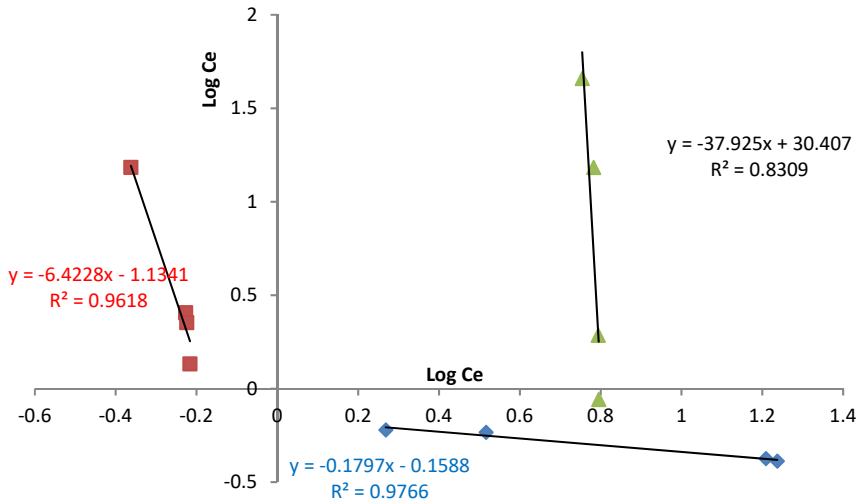

Figure 5: Freundlich plot for Fe, Cu and Ni.

The adsorption data of Fe, Ni and Cu onto MCM41 fitted the Langmuir isotherm than the Freundlich isotherm. This was because the correlation coefficients for the Langmuir isotherm were 0.9996, 0.9995 and 0.999 for Fe, Cu and Ni respectively whilst the correlation coefficients for the Freundlich isotherm were below 0.98 for all metals. The Langmuir isotherm equilibrium constant, R_L, for all metals was below 1 showing that the Langmuir adsorption was favourable [9].

3.7 Adsorption kinetics

The metal removal data was plotted into either pseudo first or second order kinetics. Figures 6 and 7 show the pseudo first or second order kinetics plots respectively.

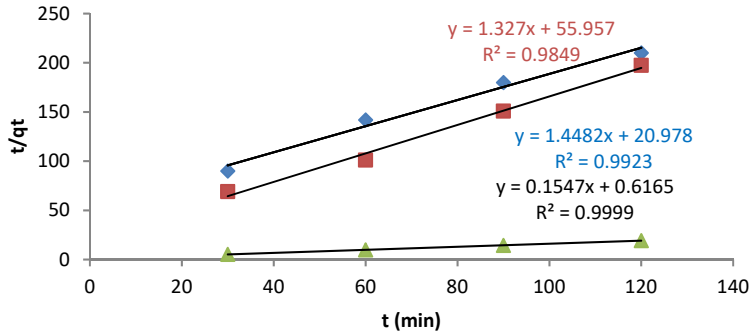

Figure 6: Pseudo second order plot for Fe, Cu and Ni.

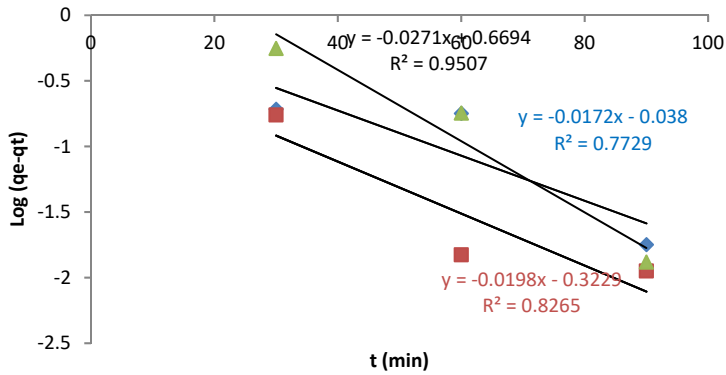

Figure 7: Pseudo first order plot for Fe, Cu and Ni.

Metal adsorption onto MCM41 fitted the pseudo second order kinetic more than the pseudo first order kinetic. This was because the correlation coefficients for pseudo first order were 0.9999, 0.9923 and 0.9849 for Fe, Cu and Ni whilst the pseudo first order coefficients were below 0.96. This is further supported by the calculated adsorption capacity vs the actual adsorption capacity. Table 4 shows the comparison of the two.

From Table 4 it can be seen that the pseudo second order calculated adsorption capacities were closer to the actual adsorption capacities as compared to pseudo first order calculated adsorption capacities. This further validates that the pseudo second order describes better the adsorption of Fe, u and Ni onto MCM41 which indicates a chemisorption process.

Table 4: A comparison of calculated and actual adsorption capacity.

Metal	Fe	Cu	Ni
Pseudo first order adsorption capacity (mg/g)	4.67	0.48	0.92
Pseudo second order adsorption capacity (mg/g)	6.46	0.69	0.75
Actual adsorption capacity (mg/g)	6.24	0.61	0.62

3.8 Effect of temperature on metal adsorption

Figure 8 shows the variation of the adsorption capacity with temperature.

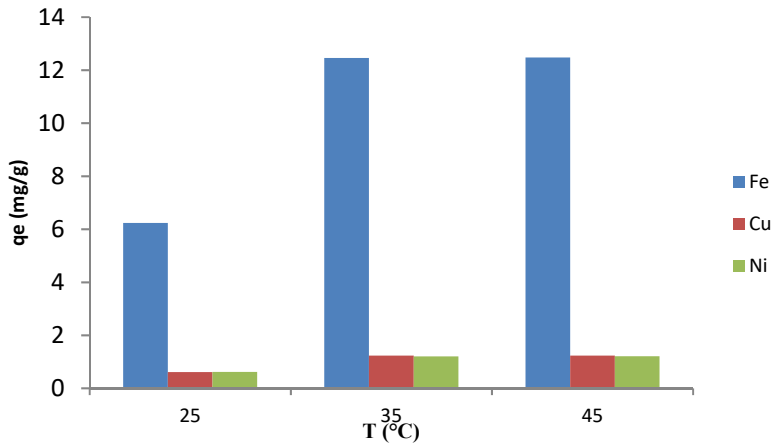

Figure 8: Variation of adsorption capacity with temperature.

There was a double increase in adsorption capacities for all metals from 25°C to 35°C, thereafter the change was statistically insignificant. The increase in adsorption capacity showed that the process was endothermic which is supported by the thermodynamic data. Figure 9 shows the Gibbs free energy plot for all the metals.

A decrease in the negative value ΔG^0 for Fe, Ni and with an increase in temperature showed that the adsorption of these metals onto MCM41 became more thermodynamically spontaneous at higher temperatures. At 45°C the Gibbs free energy for the adsorption of Fe, Cu and Ni were 4.1, 2.7 and 1.5 kJ/mol respectively. The values for enthalpy for Fe, Cu and Ni 19.97, 21.40 and 16.44 respectively showing that the adsorption process was endothermic. The values for entropy for Fe, Cu and, Ni 75.6, 76.2 and 56.5 J/mol respectively showing that MCM41 had an affinity for the metal ions in question [11].

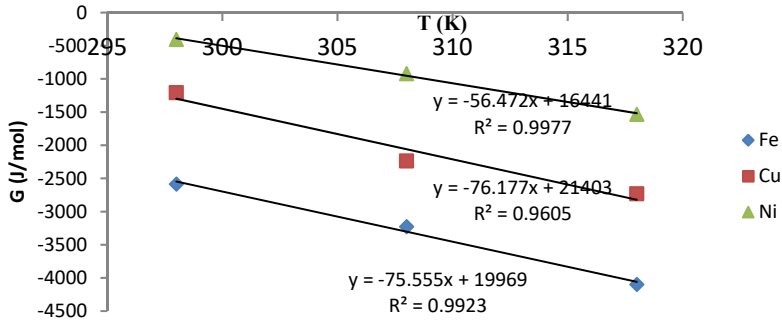

Figure 9: Gibbs free energy plot for Fe, Cu and Ni.

4 Conclusion

Potassium silicate solutions can be used as a source for MCM41. The preparation of MCM41 was affected by the gelation pH. A pH of 7 produced the purest MCM41 with a reasonable surface area. The MCM41 could be used as an adsorbent for heavy metals in AMD. The adsorption process was endothermic. The process was also thermodynamically spontaneous with the spontaneity increasing with an increase in temperature.

Acknowledgements

The authors would like to thank the University Research Council of the University of Johannesburg for their financial support. The authors are also thankful to the National Research Foundation of South Africa for providing a bursary for the student.

References

[1] Eberhard, A., The Future of South African Coal: Market, investment, and Policy challenges, Working Paper, 100, 2011.
[2] McKerall, W.C., W.B. Ledbetter, and D. J. Teague. Analysis of Fly Ashes Produced in Texas. Texas Transportation Institute, Research Report No. 240-1, Texas A&M University, College Station, Texas, 1982.
[3] Hui, K.S. and Chao, C.Y.H., Synthesis of MCM-41 from coal fly ash by a green approach: Influence of synthesis pH. *Journal of Hazardous Materials,* B137, pp. 1135–1148, 2006.
[4] Liou, T. and Lin, H., Synthesis and surface characterization of silica nanoparticles from Industrial resin waste controlled by optimal gelation conditions. *Journal of Industrial and Engineering Chemistry*, 18, pp. 1428–1437, 2012.

[5] Expert Team of the Inter-Ministerial Committee, Mine water management in the Witwatersrand Gold Fields with special emphasis on acid mine drainage. Report to the Inter-Ministerial Committee on Acid Mine Drainage, Department of Water Affairs, Pretoria, 2010.
[6] Voegtlin, A.C., Matijasic, A., Patarin, J., Sauerland, C., Grillet, Y. and Huve, L., Room-temperature synthesis of silicate mesoporous MCM-41-type materials: Influence of the synthesis pH on the porosity of the materials obtained, *Microporous Materials*, 10, pp. 137–147, 1997.
[7] Ntuli, F. and Lewis, A.E., Kinetic modelling of nickel powder precipitation by high-pressure hydrogen reduction. *Chemical Engineering Science*, 64, pp. 2202–2215, 2009.
[8] Affandi. S., Setyawan, H., Winardi, S., Purwanto, A. and Balgis, R., A facile method for production of high-purity silica xerogels from bagasse ash. *Advanced Powder Technology*, 20, pp. 468–472, 2009.
[9] Juang, R.S., Wu, F.C. and Tseng, R.L., Ability of activated clay for the adsorption of dyes from aqueous solutions: *Environmental Technology*, 18, p. 35, 1997.
[10] Gupta, V.K., Equilibrium uptake, sorption dynamics, process development, and column operations for the removal of copper and nickel from aqueous solution and wastewater using activated slag, a low-cost adsorbent. *Industrial & Engineering Chemistry Research* 37, pp. 192–200, 1998.